Green Chemistry

Life cycle energy use and greenhouse gas emissions of ammonia production from renewable resources and industrial by-products

SCHOLARONE™
Manuscripts

1   Life cycle energy use and greenhouse gas emissions of ammonia production from

2   renewable resources and industrial by-products

3   Xinyu Liu,[1] Amgad Elgowainy,[1] Michael Wang[1]

4   [1]Systems Assessment Center, Energy Systems Division, Argonne National Laboratory

5   Keywords: ammonia production, life cycle analysis, greenhouse gases, energy use

6   Abstract

7   Conventionally, ammonia is produced from natural gas via steam methane reforming (SMR),

8   water-gas shift reaction, and the Haber-Bosch process. The process uses fossil natural gas, which leads to

9   2.6 metric tons of life cycle greenhouse gas (GHG) emissions per metric ton of ammonia produced. With

10   ammonia being the second most produced chemical in the world, its production accounts for

11   approximately 2% of worldwide fossil energy use and generates over 420 million tons of CO_2 annually.

12   To reduce its carbon intensity, ammonia synthesis relying on renewable energy or utilizing by-products

13   from industrial processes is of interest. We conduct a life cycle analysis of conventional and alternative

14   ammonia production pathways by tracking energy use and emissions in all conversion stages, from the

15   primary material and energy resources to the ammonia plant gates. Of all the alternative pathways,

16   obtaining N_2 from cryogenic distillation and H_2 from low-temperature electrolysis using renewable

17   electricity has the lowest cradle-to-plant-gate GHG emissions, representing a 91% decrease from the

18   conventional SMR pathway.

19   1. Introduction

20   Ammonia is the second most produced chemical in the world nowadays.[1] Most of the ammonia

21   produced was used for nitrogen fertilizer manufacture.[2] However, research suggests ammonia as a

22   promising zero-carbon energy carrier because of its high volumetric energy density, which is

23   approximately twice as high as that of liquid hydrogen (H_2). Moreover, ammonia stays in liquid form at

24   room temperature and low pressure (~10 bar)[3]; while the liquefaction of H_2 requires cooling to -253℃ and

25   approximately 12 kWh of electricity per kilogram (kg) of H_2 produced.[4] The safe handling and

26   transportation infrastructure of ammonia are already in place, which may facilitate the transformation to

27   an expanded ammonia-based energy sector.[5]

28   Ammonia is also being explored for long-term energy storage to enable greater penetration and

29   utilization of intermittent renewable wind and solar energy sources.[5] Ammonia can play an essential role

30   in a future energy landscape with increased penetration of renewables by balancing the temporal

31   discrepancy between the supply of and demand for energy in various regions.

32   With these emerging applications of ammonia, future global production for ammonia could

33   increase by orders of magnitude.[5] Conventionally, ammonia is produced from steam methane reforming

34   (SMR) of fossil natural gas or gasification of coal; these account for 72% and 22% of global ammonia

35   production capacity, respectively.[1] Other feedstocks for ammonia production include fuel oil (4%) and

36   naphtha (1%).[6] Ammonia production accounts for approximately 2% of worldwide fossil energy use and

37   generates over 420 million tons of CO_2 annually, representing 1.2% of the global anthropogenic CO_2

38   emissions.[1,5] To decarbonize the ammonia sector, alternative ammonia production pathways from

39   renewable sources are of increasing interest.

40   With current technologies, it is feasible to produce ammonia from carbon-free resources — water

41   and air — using renewable electricity as the main energy source for air separation and water

42   electrolysis.[5,7] For example, a commercial plant recently built by Yara, a nitrogen fertilizer manufacturer,

43   demonstrated the use of renewable electricity to split water into H_2 and O_2 and the Haber-Bosch (HB)

44   reaction to combine H_2 and N_2 to produce low-carbon ammonia.[8] Morgan et al. conducted two techno-

45   economic analyses of wind-powered ammonia production to demonstrate the process's economic

46   feasibility.[3,7]

47   One of the most-used techniques for environmental assessment of any product is life cycle

48   analysis (LCA). LCA holistically evaluates the environmental impacts of a product by compiling an

49   inventory of energy and material inputs to the various stages along the product's life cycle and calculating

50   the associated resource use and resulting emissions. [9]

51   LCA has been widely applied to evaluate conventional ammonia production pathways. [10,11]

52   Johnson et al. assessed the life cycle energy use and greenhouse gases (GHG) emissions from SMR of

53   fossil natural gas in the U.S., using industry-aggregated inventory data [10]. Zhang et al. quantified the life

54   cycle GHG emissions resulting from China's nitrogen fertilizer production and consumption supply

55   chain, with a focus on using prevailing technologies to produce ammonia, such as natural gas SMR and

56   coal gasification.[11] Bicer et al. assessed the use of fossil resources, such as coal, natural gas, and heavy

57   oil, to produce ammonia and reported the global warming potential (GWP) for a period of 500 years.[12]

58   They concluded that using electricity generated from fossil resources for H_2 production via water

59   electrolysis would incur more life cycle GHG emissions than the natural gas SMR pathway.

60   Only few studies applied LCA to assess alternative low-carbon ammonia production pathways,

61   although alternative low-carbon ammonia production technologies utilizing renewable electricity have

62   been extensively studied [3,7,13–16]. Bicer et al. compared the life cycle energy and exergy efficiency, as well

63   as the GHG emissions, of various ammonia production pathways employing the HB reaction and H_2 from

64   water electrolysis and using zero- or low-carbon electricity from municipal waste, nuclear, biomass, and

65   hydropower.[6] In another LCA study, Bicer and Dincer evaluated the impacts of different end-use

66   applications of ammonia produced from an electrochemical pathway, such as city transportation and

67   power generation [17]. In these two LCA studies, H_2 was assumed to be produced from water electrolysis

68   and N_2 from cryogenic distillation [6,17]. However, other large-scale potential sources of H_2 have not been

69   assessed, for example, H_2 as industrial by-products [18,19]. Moreover, other air separation techniques have

70   not been analyzed.

71   In this paper, we extend the work of Bicer et al. and Zhang et al. by using LCA to assess

72   additional low-carbon technology pathways to produce syngas containing the N_2 and H_2 needed by the

3

73 HB loop for ammonia synthesis. We evaluate two technologies for producing N_2: cryogenic distillation

74 (CD) and pressure swing adsorption (PSA), and four technology pathways to produce H_2: low-

75 temperature electrolysis (LTE), high-temperature electrolysis (HTE), as a by-product from chlor-alkali

76 (CA) processes, and as a by-product in steam cracker (SC) plants. In addition, this work provides a

77 detailed energy and emission inventory for each stage in the ammonia life cycle for each of the

78 technology pathways considered. This work also assesses the sensitivity of energy use and GHG

79 emissions to the source of electricity, key process parameters, and co-product treatment methods.

2. Ammonia manufacturing technology description and evaluation of system

80

81 boundary

82 Our LCA system boundary is cradle-to-plant-gate, and the functional unit is 1 metric ton of

83 ammonia produced. We utilized the Greenhouse gases, Regulated Emissions, and Energy use in

84 Technologies (GREET®) model (2019) to conduct the LCA.[20,21] We evaluate energy use and GHG

85 emissions associated with ammonia production pathways, here referred to as the "cradle-to-plant-gate life

86 cycle." Those related to equipment manufacturing, e.g., reactors or electrolytic cells, are likely to be small

87 considering the ammonia throughput over the life of a production plant, and are thus kept out of scope for

88 this analysis. The goal is to evaluate the life cycle GHG emissions of ammonia produced from alternative

89 low-carbon pathways in comparison with the conventional natural gas SMR pathway.

90 We assume that the H_2 plant, N_2 plant, and HB plant are co-located. Moreover, since our study of

91 the ammonia production pathways ends at the ammonia plant gate, the storage, transportation, and end

92 use of ammonia are not included in the scope of analysis. The cradle-to-plant-gate GHG emissions are

93 presented in CO_2 equivalents (CO_{2e}) of CO_2, CH_4, and N_2O with their 100-year GWP of 1, 30, and 265,

94 respectively, following the Intergovernmental Panel on Climate Change (IPCC) Fifth Assessment

95 Report.[22]

Conventional ammonia production based on steam methane reforming

Conventionally, ammonia is produced from SMR of natural gas. There are two main functional steps in this pathway: The first is to produce H_2 from natural gas via steam methane reforming, and the second is to synthesize ammonia via the HB process, as depicted in Figure 1. In the natural gas supply in North America, which is the focus of this study, the shares of conventional and shale gas are 48% and 52%, respectively.[20]
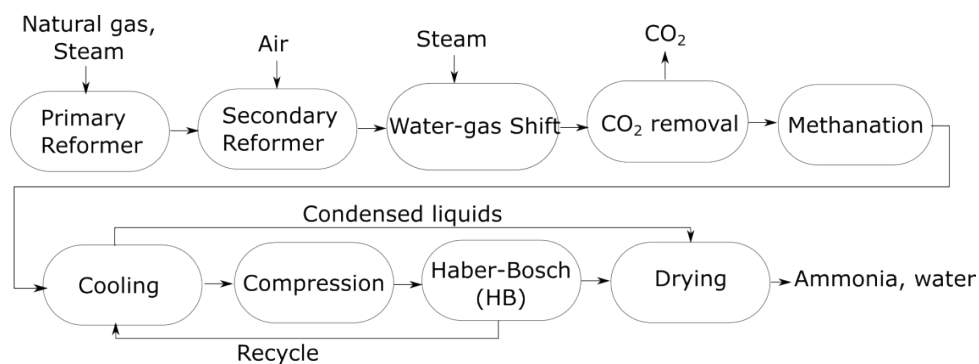
Figure 1: Process diagram for conventional ammonia production (adapted from Johnson et al.[10])

Methane (CH_4) is reformed with steam at up to 1000°C in the primary and secondary SMR reactors to form H_2 and carbon monoxide (CO) according to Reaction 1:

$$CH_4 + H_2O \rightarrow CO + 3H_2 \tag{1}$$
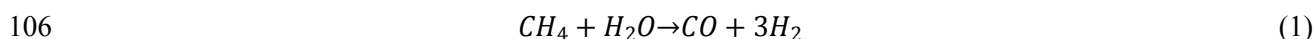
Compressed air is introduced into the secondary SMR reactor to combust a portion of the natural gas to provide heat of reaction.[10] Oxygen (O_2) is depleted during the combustion, while the stoichiometric nitrogen (N_2) is used in the downstream HB synthesis loop, avoiding the need for an air separation unit (ASU) in this pathway. The gas mixture at the SMR reactor outlet contains H_2, CO, CO_2, unreacted steam, and CH_4, and is cooled and sent to a two-stage water-gas shift (WGS) reactor to increase the H_2 yield, according to Reaction 2:

$$CO + H_2O \leftrightarrow CO_2 + H_2 \tag{2}$$
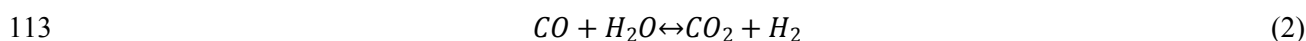
Mono-ethanol-amine scrubbing or the Selexol process is employed to remove CO_2, and methanation converts the remaining CO into CH_4 to prevent poisoning of the HB catalyst. After

116   compression, the syngas mixture enters the HB loop, where stoichiometric N_2 and H_2 react at 150–250 bar

117   and 400°C–450°C with the presence of iron-based catalyst to produce ammonia according to Reaction 3:[5]

118    $$N_2 + 3H_2 \rightarrow 2NH_3 \tag{3}$$
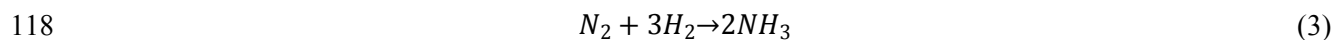
119   Recycling is needed, since the single-pass conversion rate for ammonia is low (around 15%).

120   Ammonia is condensed and separated at -25°C to -33°C. The unreacted N_2 and H_2 are compressed and

121   recycled to the HB reactor. Heat recovered from the cooling of the gas mixture exiting the secondary

122   SMR reactor is used to raise the temperature of the steam, which is expanded in the steam turbine to drive

123   the compression of air fed into the secondary SMR reactor and feed gas introduced to the HB synthesis

124   loop. Therefore, the modern ammonia manufacturing process is highly integrated.

125   The inventory of this integrated pathway was incorporated into the GREET model, as

126   summarized in Table 1, and used for this analysis without modification.[20] The cradle-to-plant-gate GHG

127   emissions for this pathway are 2.6 metric ton CO_{2e}/metric ton ammonia,[20,23] which agrees well with the

128   range reported in Zhang et al. (2.1–3.6 metric tons CO_{2e} per metric ton NH_3).[11] For comparison, the

129   cradle-to-plant-gate GHG emission of the coal gasification pathway to produce ammonia is 6.1–7.8

130   metric tons CO_{2e} per metric ton NH_3, which is much higher than the natural gas SMR pathway.[11] Our

131   results are less comparable with those in Bicer et al.,[12] since they reported the GWP for a period of 500

132   years while we calculated the 100-year GWP.

133   ## Alternative ammonia production

134   In addition to the natural gas SMR pathway, there are alternative technologies for ammonia

135   manufacturing. The basic structure of these alternative pathways is depicted in Figure 2. High purity N_2 is

136   obtained by separating air, and high purity H_2 can be produced from various technologies, as explained

137   below.
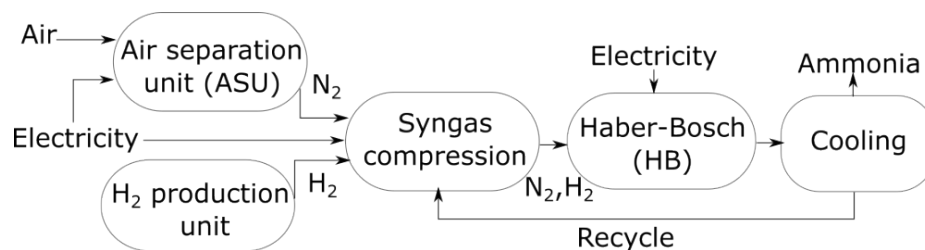
The gas mixture containing stoichiometric N_2 and H_2 is compressed to the operating pressure of the HB reactor (assumed to be 200 bar in this analysis) and enters the electricity-driven HB synthesis loop. As with the conventional pathway, the single-pass conversion rate for ammonia is only 15%, so recycling of unreacted syngas is needed. There is a pressure drop around the HB synthesis loop, which is assumed to be 6% of the operating pressure of HB reactor.[3,24] Thus, for a HB reactor pressure of 200 bar, the single-pass pressure drop is approximately 12 bar. To overcome this pressure drop, the recycled gas mixture needs to be recompressed to the operating pressure of the HB reactor. In the HB synthesis loop, the electricity is required almost exclusively for syngas/recycle gas compression.[3,7] The synthesis loop does not need an external heat source, since the HB reaction is exothermic, and the utilization of reaction heat through heat integration is sufficient to satisfy the process heat demand.[14,25] Pumping energy is also required to circulate cooling water. According to Morgan et al.,[7] the pumping power only accounts for ~1% of the total power required in the synthesis loop, so it is considered negligible and not included in this analysis.

It is worth mentioning that the HB loop, including the syngas compression, needs to be supplied with constant power. Therefore, in this analysis, we assume that the HB loop utilizes grid electricity to power the electric motors that drive gas compressors. For a large pressure increase, a multi-stage compressor should be used with an intercooler between stages to reduce the compression power and keep the compression discharge temperature below a practical limit. Equation 4 is applied to calculate the compression energy:

159
$$E_{comp} = \frac{1}{3600} \times \frac{1}{\eta_{EM}} \times n \times Z \times R \times T \times \frac{1}{\eta_C} \times \frac{k}{k-1} \times \left[\left(\frac{P_{outlet}}{P_{inlet}} \right)^{\left(\frac{k-1}{nk} \right)} - 1 \right]$$
(4)

160 where E_{comp} is the energy required for gas compression in the unit of kWh/kg gas, η_{EM} is the electric

161 motor efficiency, assumed to be 95% in this analysis, and n is the number of compression stages,

162 determined by the outlet pressure (P_{outlet}, in units of bar or psi), the inlet pressure (P_{inlet}, in the unit of bar

163 or psi), and the compression pressure ratio per stage. In this analysis, we assume the per-stage

164 compression ratio is 2 for both N_2 and H_2. Z is the compressibility factor, assumed to be 1 in this analysis,

165 R is the gas constant (0.297 kJ/kg-K for N_2, 4.125 kJ/kg-K for H_2, and 0.978 kJ/kg-K for syngas), T is the

166 inlet gas temperature in degrees Kelvin, η_C is the isentropic efficiency of compression, assumed to be

167 80% in this analysis, and k is the specific heat ratio (1.4 for N_2 and H_2).

168 Applying Equation 4, the electric energy required by the HB loop is 0.324 kWh/kg NH_3. This

169 value is comparable to those reported in literature. Frattini et al. reported a compression power demand of

170 0.44 kWh/kg NH_3 using an Aspen Plus simulation,[14] while Morgan et al. reported the energy required by

171 the HB synthesis loop to be approximately 0.64 kWh/kg NH_3 based on literature values.[7,24] These

172 differences may stem from the variations in process specifications: pressures at which syngas N_2 and H_2

173 are produced, assumed compression efficiency, assumed electric motor efficiency, pressure of the HB

174 reactor, and pressure drop in the HB loop.

175 ## Various technologies for N_2 production from air separation

176 There are three main methods of separating N_2 from air: cryogenic distillation, pressure swing

177 adsorption (PSA), and membrane separation. Membrane separation cannot achieve a purity level high

178 enough for ammonia production, especially at a high flowrate[14] and without a deoxygenator.[7] Moreover,

179 O_2 cannot be recovered as a co-product with membrane separation.[26] Therefore, we focus on the other two

180 technologies in this analysis.

181   *Cryogenic distillation*

182   Cryogenic distillation accounts for more than 90% of the global production of N_2.[26] It is suitable

183   for large system production with impurity concentrations down to the parts-per-billion range.[26] Compared

184   to other air separation methods, cryogenic distillation produces the purest N_2 and requires the smallest

185   input power.[26] Cryogenic distillation works by utilizing the differences in boiling point of major air

186   components: Air is cooled down to its dew point while the contaminants are removed, and then distilled

187   into its individual components with a distillation column. The energy requirement for separating one

188   standard cubic meter of pure N_2 at 8 bar ranges from 0.15 to 0.25 kWh, which is bound by two

189   modifications to the double-column system. In this analysis, we use a mid-value of 0.2 kWh/m^3 at

190   standard temperature (0 °C) and pressure (1 bar) (STP). With the density of N_2 at STP equal to 1.23

191   kg/m^3, 162 kWh of electricity is consumed per metric ton N_2 produced.[26] Since the liquefaction of air

192   occurs at low temperatures and requires a steady energy supply, we assume for the base design case that

193   the cryogenic distillation of air to produce N_2 utilizes grid electricity.

194   *Pressure swing adsorption*

195   PSA is suitable for small system production, with N_2 purity up to 99.99%.[26] A N_2-PSA plant

196   utilizes carbon molecular sieves, which in the adsorption mode preferably adsorb H_2O, CO_2 and O_2 while

197   letting N_2 pass through into a buffer tank. In the adsorbent regeneration mode, the pressurized gas in the

198   adsorber is released to the atmosphere. The N_2 collected in the buffer tank serves as the final product.

199   The PSA unit is more flexible in the context of renewable energy utilization, since it only needs a

200   few minutes to reach its full production capacity. This feature is particularly useful when the energy

201   supply for producing N_2 fluctuates significantly, as is the case with intermittent renewable energy. In

202   contrast, the cryogenic ASU needs two hours before it starts to steadily produce N_2 and O_2. It is estimated

203   that 365 kWh of electricity is required to produce a metric ton of nitrogen at 8 bar, which is a typical

204   operating pressure for N_2-PSA unit.[26]

205   ## Various technologies for H$_2$ production

206   Four alternative H$_2$ production technologies are evaluated in this study, all of which satisfy the H$_2$

207   purity requirement for the HB process and supply H$_2$ at 20 bar.[20]

208   *By-product H$_2$ from chlor-alkali processes*

209   H$_2$ may be available as a by-product from the chlor-alkali (CA) process, which coproduces

210   sodium hydroxide and chlorine as main products via electrolysis of a sodium chloride solution. Reactions

211   5 and 6 occur at cathode, while 7 and 8 occur at anode. Reaction 9 represents the overall reaction.[27]

212     $$2H_2O + 2e^- \rightarrow H_2 + 2OH^- \tag{5}$$

213     $$2Na^+ + 2OH^- \rightarrow 2NaOH \tag{6}$$

214     $$2NaCl \rightarrow 2Na^+ + 2Cl^- \tag{7}$$

215     $$2Cl^- \rightarrow Cl_2 + 2e^- \tag{8}$$

216     $$2NaCl + 2H_2O \rightarrow Cl_2 + 2NaOH + H_2 \tag{9}$$
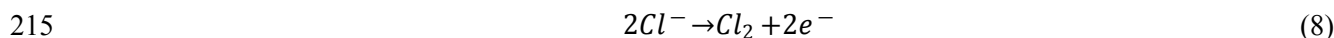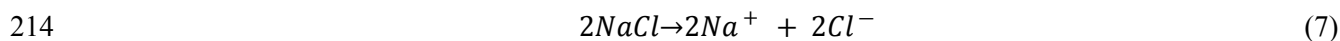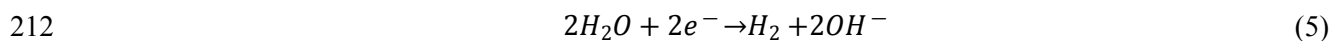
217   Hydrogen as a by-product from CA plants is vented if not sold for industrial use.[19,20] The CA

218   process is a mature industrial technology capable of co-producing high-purity H$_2$ on a large scale (up to ~

219   0.4 million tons per year) and at a relatively low price (~ \$1/kg H$_2$).[19] H$_2$ produced from the CA process is

220   of high purity (>99.9%), obviating the need for an additional purification process. Therefore, the post-

221   processing of H$_2$ only requires cooling/drying and compression. From a H$_2$ production standpoint,

222   electricity is needed for electrolysis of the sodium chloride solution and compression of H$_2$, while heat is

223   required to process the sodium chloride solution. Electricity can be sourced from the grid or an onsite

224   combined heat and power (CHP) system. If the CA process has a CHP system, then the process heat

225   demand can be met solely by the recovered heat from the CHP. Otherwise, the process heat is provided by

226   natural gas boilers. A detailed process inventory is available in Lee et al., where four H$_2$ co-product

227   treatment methods are assessed: venting, combustion/substitution, mass allocation, and market value

228   allocation.[19,27] In this study, we assume that there is no on-site CHP and consider three treatments of by-

229   product H_2 — venting (as the base design case), combustion/substitution and mass allocation (as

230   sensitivity cases) — which cover the two extremes in terms of cradle-to-plant-gate GHG emissions. If the

231   CA plant is designed to vent by-product H_2, it is treated as waste. However, if the CA plant is designed to

232   use byproduct H_2 for process heat, then the thermal energy in the H_2 exported for ammonia production

233   must be replaced by an equivalent thermal energy, which we assume to be sourced from natural gas.

234   *By-product H_2 from steam cracking of natural gas liquids (NGLs)*

235   By-product H_2 from the steam cracking (SC) of NGLs has been of interest recently due to

236   increased shale gas production. It is estimated that 3.5 million tons of by-product H_2 can be available

237   annually from steam cracker plants.[18] Steam cracker plants use thermal cracking of hydrocarbon

238   feedstock, such as NGLs, to produce light olefins and other co-products. As shown in Reaction 10, H_2 is

239   available as a by-product of the cracking process.

240
$$C_nH_{2n+2} + steam \xrightarrow{heat} aH_2 + bCH_4 + cC_2H_4 + dC_3H_6 + eC_4H_8 + fC_{5+} \qquad (10)$$

241   The heat required for cracking is usually provided by combusting a mixture of by-product H_2,

242   natural gas, and/or surplus CH_4 from the cracking process. Alternatively, by-product H_2 may be separated

243   for export to other markets (e.g., ammonia production), and its heating value can be replaced with

244   combusting additional natural gas. The cracked gas is usually post-processed through quenching,

245   compression, and fractionation to separate the mixture into individual products. PSA can be employed to

246   separate and purify by-product H_2 to meet the requirements of the HB process. The energy intensity of the

247   PSA unit is estimated at 0.5 kWh/kg H_2. A detailed process inventory is available in Lee et al.[18]

248   Two co-product treatment methods are considered: substitution (as the base case) and mass

249   allocation (as a sensitivity case). The substitution method is similar to what has been described above for

250   the CA process, since most steam cracker plants combust by-product H_2 on site for process heat. For mass

251   allocation, the mass balance between products is used to allocate environmental burdens.

252   *Low-temperature electrolysis (LTE) from renewable electricity*

253   There are two common water electrolyzer technologies used in low-temperature applications:

254   alkaline and proton exchange membrane (PEM). Both are mature technologies and have the potential to

255   produce H_2 at a large scale, but the latter is more suitable for use with intermittent renewables due to its

256   fast response rate.[5,16]

257   As its name suggests, alkaline electrolysis employs a 25%–30% aqueous KOH solution as the

258   electrolyte in which the electrodes are immersed, separated by a diaphragm.[28] Reactions 11 and 12

259   represent the reactions occurring at the cathode and anode, respectively, with a direct current application:

260 $$2H_2O + 2e^- \rightarrow H_2 + 2OH^- \tag{11}$$

261 $$2OH^- \rightarrow \frac{1}{2}O_2 + H_2O + 2e^- \tag{12}$$
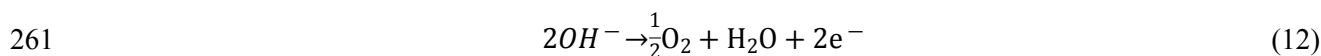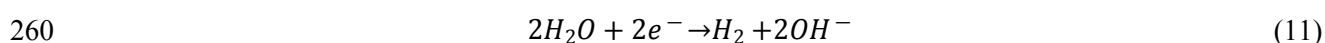
262   H_2 is produced at the cathode with a high purity, typically ranging from 99.5%–99.9% after drying. The

263   system energy efficiency of the alkaline electrolyzer is in the range of 51%–60% based on the lower

264   heating value of H_2.

265   PEM electrolysis utilizes a solid proton-conducting membrane stack on which the electrodes are

266   usually directly mounted. Reactions 13 and 14 represent the reactions taking place at the cathode and

267   anode, respectively. Both reactions happen in the acidic regime, in contrast to those of alkaline

268   electrolysis.

269 $$2H^+ + 2e^- \rightarrow H_2 \tag{13}$$

270 $$H_2O \rightarrow \frac{1}{2}O_2 + 2H^+ + 2e^- \tag{14}$$
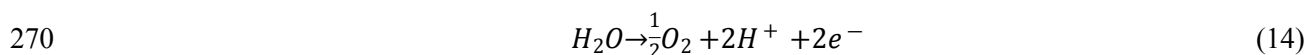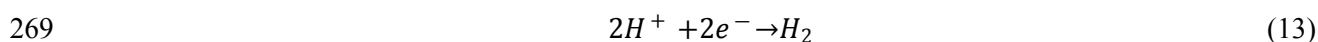
271   PEM electrolysis produces H_2 at the cathode with a purity over 99.99%, due to the very low

272   permeation across the PEM. A PEM electrolyzer cell can operate under higher current density (>1500

273   milliamps per square centimeter [mA/cm^2]) than the alkaline electrolyzer cell (200-600 mA/cm^2), which

274   supports the higher-pressure operation of PEM electrolysis and reduces the downstream burden to

275   compress the syngas at the HB reactor.[16,28]

276   PEM electrolyzer technology has an energy efficiency of up to 72%.[20] In this analysis, we assume

277   that PEM electrolyzer energy efficiency is 63% based on a lower heating value of H_2, meaning that 63%

278   of the input electric energy would be stored in the H_2 product in the form of chemical energy (lower

279   heating value).[29] The electricity for electrolysis is assumed to be sourced from renewable resources, such

280   as wind or solar. However, to balance the supply and demand of intermittent and geographically isolated

281   renewable electricity, storage equipment, such as an H_2 storage tank and/or battery, is needed to enable a

282   consistent H_2 supply to the HB loop. This may increase the capital investment and impact the cost of the

283   ammonia produced, which is beyond the scope of this analysis.

284   *High-temperature electrolysis with solid oxide electrolysis cell*

285   A solid oxide electrolysis cell (SOEC) is used for high-temperature electrolysis (HTE)

286   applications due to its ability to withstand high temperatures. H_2 production from high-temperature

287   electrolysis using SOEC provides higher electrical energy efficiency than low-temperature electrolysis,

288   since part of the total process energy requirement is satisfied by heat rather than electricity.[6] In this

289   analysis, we assume that the required heat and electricity are provided by a high-temperature gas-cooled

290   reactor (HTGR) using uranium (U-235) as fuel. The upstream energy use and emissions associated with

291   uranium mining, conversion, enrichment, and transportation are estimated by the GREET model.[20,30] In

292   the HTGR, heat is generated to increase the temperature of steam entering the SOEC to approximately

293   800°C. The remaining heat drives a high-efficiency gas turbine to produce electricity for the electrolysis

294   process. Reactions 15 and 16 represent the reactions at the cathode and anode of SOEC, respectively.[28]

$$H_2O + 2e^- \rightarrow H_2 + O^{2-} \tag{15}$$

$$O^{2-} \rightarrow \tfrac{1}{2}O_2 + 2e^- \tag{16}$$
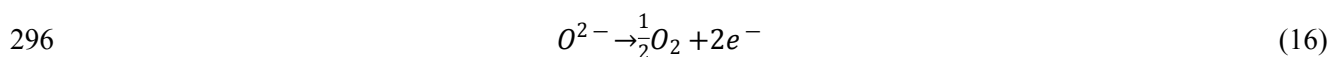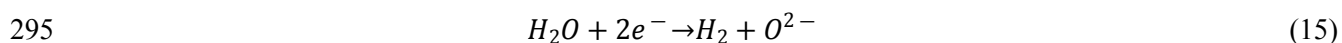
297   H_2 is produced at the cathode and separated from the steam by cooling and condensation of water.

298   For both water electrolysis pathways, LTE and HTE, the overall reaction is the same and is given

299   by Reaction 17:

$$H_2O \xrightarrow{\text{electricity}} H_2 + \frac{1}{2}O_2 \qquad (17)$$
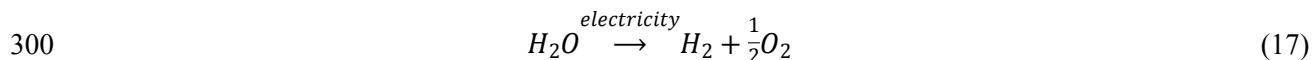
According to the reaction stoichiometry, when producing 1 kg of H_2, 7.9 kg of O_2 is produced as a by-product. In this analysis, no credits have been given to by-product O_2 from N_2 production from air or H_2 production from water.

Table 1: Inventories for conventional and alternative ammonia production

Technologies	Electricity (GJ)	Natural gas (GJ)	N$_2$ @ 8 bar (metric ton)	H$_2$ @ 20 bar (metric ton)	Energy efficiency
Ammonia production (per metric ton NH$_3$)					
Integrated conventional ammonia production based on SMR	0.47	36.5*	-	-	
N$_2$ production (per metric ton N$_2$)					
Cryogenic distillation	0.584	-	-	-	
Pressure swing adsorption	1.313	-	-	-	
H$_2$ production (per metric ton H$_2$)					
Electrolysis of sodium chloride solution	6.225	-	-	-	
Steam cracking of NGLs	1.8	120	-	-	
Low-temperature PEM electrolysis	190	-	-	-	63%
High-temperature solid oxide electrolysis	-	-	-	-	50%**
Ammonia production (per metric ton NH$_3$)					
Electric-based Haber-Bosch	1.165	-	0.822	0.178	

* 28.3% of the total natural gas input is used as fuel.
** A thermal-to-hydrogen efficiency of 50% is used.[31]

3. Results and Discussion

Cradle-to-plant-gate fossil energy consumption

Figure 3 shows the cradle-to-plant-gate fossil energy consumption for various ammonia production pathways. The conventional SMR pathway consumes the highest amount of fossil energy because it uses mainly fossil natural gas as feedstock and process fuel.
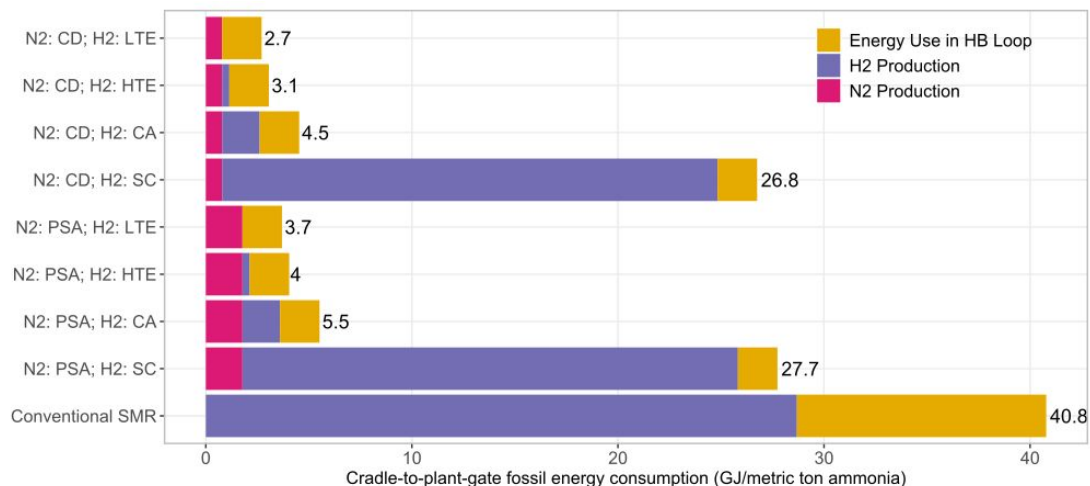
Figure 3: Cradle-to-plant-gate fossil energy consumption in base case co-product treatment methods. Electricity source for N_2 production and HB loop: 2019 U.S. grid generation mix. "Energy use in HB loop" represents the fossil energy consumed for producing and using natural gas and/or electricity in the HB loop.

For the alternative ammonia production pathways, preparing syngas via N_2-CD and H_2-LTE consumes the least fossil energy per metric ton of NH_3 produced, a 93% reduction from the conventional SMR pathway. This is because most of the energy in this pathway is required for H_2 production, and we assume that renewable electricity generated from solar or wind is used for this process. The majority of the energy consumed when producing H_2 via HTE is also non-fossil, since this process utilizes nuclear energy for both heat and power. For H_2 produced from the CA process, more fossil energy is consumed than in water electrolysis, which sources renewable electricity, since the U.S. grid mix is assumed to be used in the CA process for the cooling/drying and compression of H_2. Of the 2019 U.S. grid mix, 63% is generated from fossil resources — coal and natural gas. A significantly higher amount of fossil energy is consumed in the H_2-SC pathways as a result of the substitution method used to evaluate by-product H_2 in the base case, as mentioned earlier. In that method, natural gas combustion is assumed to substitute for the heat loss resulting from selling byproduct H_2. However, even in this scenario, the ammonia production consumes 32% less fossil energy than the conventional SMR pathway.

330 ## Cradle-to-plant-gate GHG emissions

331   Figure 4 depicts the cradle-to-plant-gate GHG emissions for various ammonia production

332 pathways.
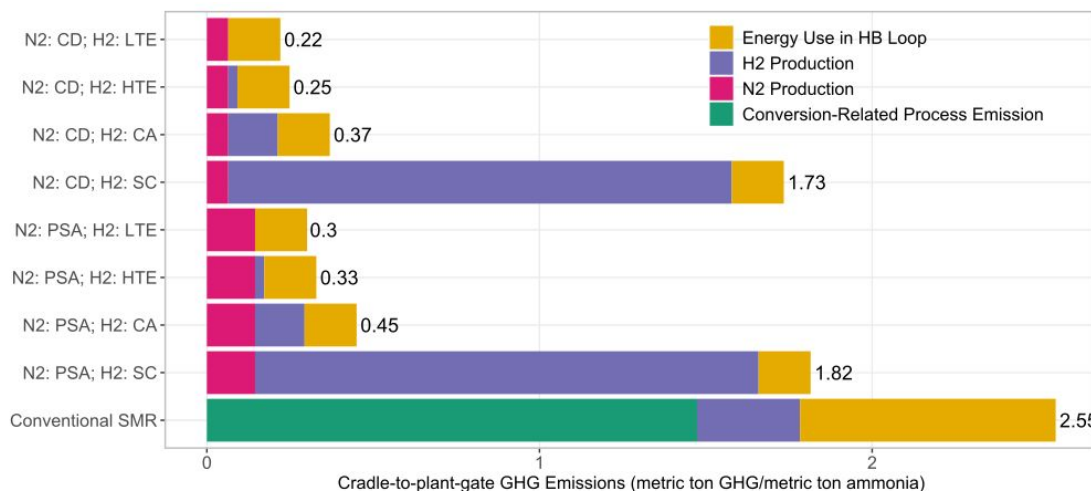
333

334 Figure 4: Cradle-to-plant-gate GHG emissions in base case co-product treatment methods. Electricity source for N_2
335   production and HB loop: 2019 U.S. grid generation mix. The "conversion-related process emission" from the
336 conventional SMR pathway consists of CO_2 generated from WGS reactor per Reaction 2. "Energy use in HB loop"
337   represents the emissions associated with producing and using energy in the HB process, which includes GHG
338   emissions from natural gas combusted in industrial boilers to provide process heat.

339   Figure 4 shows that all alternative pathways generate lower cradle-to-plant-gate GHG emissions

340 than the conventional SMR pathway. Of all the alternative pathways, obtaining N_2 from cryogenic

341 distillation and H_2 from LTE using renewable electricity has the lowest cradle-to-plant-gate GHG

342 emissions, representing a 91% decrease from the conventional SMR pathway.

343   The contribution of N_2 production to cradle-to-plant-gate GHG emissions varies among different

344 ammonia production pathways. For the pathway where N_2 production has the highest contribution to the

345 cradle-to-plant-gate GHG emissions (N_2-PSA and H_2-LTE), it accounts for 48% of the total emissions.

346 This is because producing N_2 via PSA is more energy intensive than cryogenic distillation (Table 1) and

347 H_2 produced from renewable electricity powered LTE does not contribute to GHG emissions. It is

348 noteworthy that for the conventional SMR pathway, N_2 in the syngas is not produced with ASU but by

16

349   depleting the O_2 in the air during natural gas combustion for process heat, and thus does not explicitly

350   contribute to cradle-to-plant-gate GHG emissions.

351   In this analysis, we assume that all the alternative pathways use a common HB process to produce

352   NH_3, which consumes 1.165 GJ of U.S. grid electricity per metric ton NH_3 and leads to 0.156 metric tons

353   GHG/metric ton NH_3. For pathways where H_2 is produced mainly from non-fossil sources (LTE and

354   HTE), this emission translates into a 48% to 71% contribution to the cradle-to-plant-gate GHG emissions.

355   However, if H_2 is a by-product from the steam cracker plant under the substitution co-product treatment

356   method, this emission contributes only 9% to the overall life cycle emissions.

Sensitivity analysis

357

Regional electricity generation mix

358

359   Figure 5 shows the impact of the regional utility grid generation mix on the cradle-to-plant-gate

360   GHG emissions for ammonia production. Here, we assume that N_2 is produced via cryogenic distillation

361   and ammonia is produced via HB using the regional grid generation mix. For electricity consumed in

362   various H_2 production pathways (e.g., H_2-CA and H_2-SC), we also assume that regional grid generation

363   mix is used.

364   There are eight major electricity regions in the contiguous U.S., which have different shares of

365   electricity generation technologies. The GHG emission intensity of different regional grid generation

366   mixes is shown in Figure 5. A lower GHG emission intensity for the electricity generation mix results in

367   lower cradle-to-plant-gate GHG emissions for ammonia.

368   Figure 5 demonstrates that if the Northeast Power Coordinating Council (NPCC) grid mix is used

369   to prepare syngas via N_2-CD and H_2-LTE, instead of the U.S. average grid mix, the cradle-to-plant-gate

370   GHG emission per metric ton of ammonia produced can be reduced by 44%. This is because the NPCC

371   grid has the largest share of near-zero-carbon nuclear and hydro power generation of all utility regions.[20]
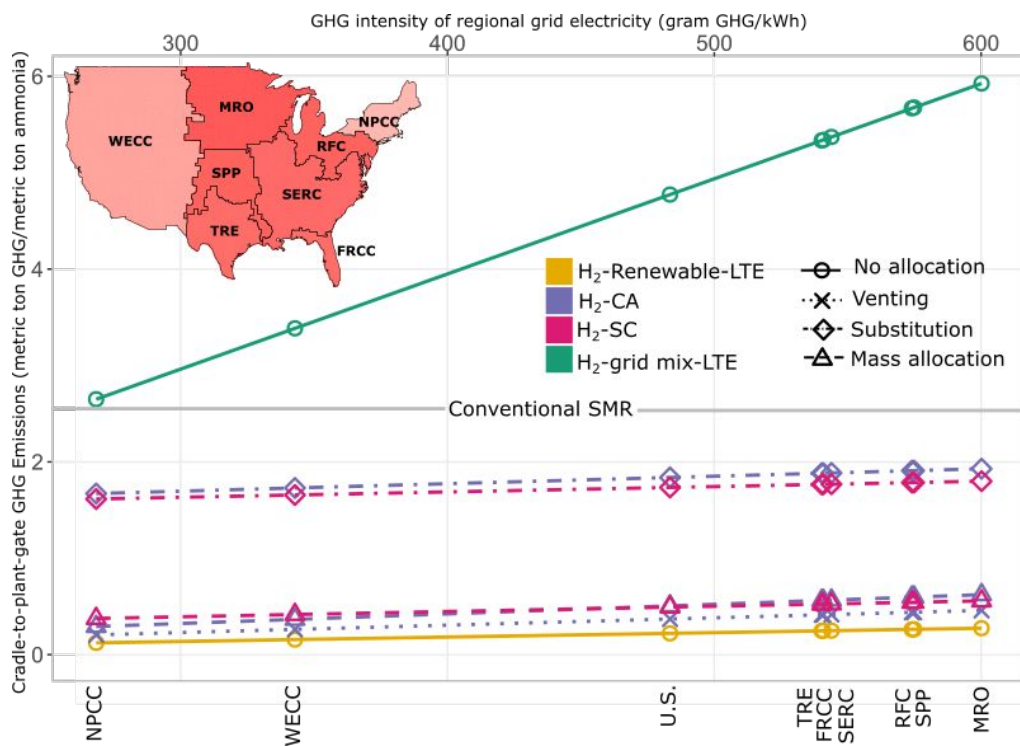
372
373   Figure 5: Impact of regional electricity grid generation mix and co-product treatment method on cradle-to-plant-gate
374   GHG emissions of various ammonia production pathways. The grey horizontal line represents the cradle-to-plant-
375   gate GHG emissions of the conventional SMR pathway in the context of 2019 U.S. grid generation mix. Regional
376   electric grids: Western Electricity Coordinating Council (WECC), Midwest Reliability Organization (MRO),
377   Southwest Power Pool (SPP), Texas Reliability Entity (TRE), SERC Reliability Corporation (SERC), Florida
378   Reliability Coordinating Council (FRCC), Reliability First Corporation (RFC), and Northeast Power Coordinating
379   Council (NPCC).

380   Figure 5 also shows that if grid electricity is used to produce H_2 via LTE (H_2-grid mix-LTE), the

381   cradle-to-plant-gate GHG emissions would increase by a factor of 21 over using renewable electricity

382   from solar/wind to power H_2-LTE, exceeding those from the conventional SMR pathway. This finding

383   suggests using electricity generated mainly from fossil resources to electrolyze water to produce H_2

384   needed for the HB process would increase life cycle GHG emissions compared to the natural gas SMR

385   pathway, which agrees well with previous findings in the literature.[12]

386   Therefore, the carbon intensity of the electricity used to power all processes in the ammonia

387   production pathway is crucial for the cradle-to-plant-gate GHG emissions associated with ammonia

388   production. In this analysis, we assume that grid electricity is used to power N_2-CD and ammonia-HB,

389   since these processes require a steady energy supply to operate in the continuous mode. The cradle-to-

390   plant-gate GHG emissions of ammonia can be further reduced if renewable electricity can be supplied

391   continuously to provide the energy required by N_2 production and the HB synthesis loop. In that case, the

392   ammonia produced can be carbon-free. However, mitigating the intermittency of renewable resources

393   such as wind and solar would require energy storage, which impacts the economics of their supply and

394   thus the economics of ammonia production.

395   ## Co-product treatment methods for H_2 production

396   Figure 5 also illustrates the impact of the H_2 by-product treatment method on the cradle-to-plant-

397   gate GHG emissions for various ammonia production pathways.

398   For byproduct H_2 from CA plants, using the substitution co-product treatment method results in

399   higher cradle-to-plant-gate GHG emissions (1.84 metric tons GHG/metric ton ammonia) than the venting

400   treatment (0.37 metric ton GHG/metric ton ammonia), due to the additional natural gas used to substitute

401   for the energy in the exported H_2. Employing mass allocation instead of venting slightly increases the

402   cradle-to-plant-gate GHG emissions (0.51 metric ton GHG/metric ton ammonia). This is because instead

403   of being treated as a waste, as in mass allocation, the environmental burdens of the CA plant are

404   distributed between sodium hydroxide, chlorine, and H_2 based on their mass shares in the total plant mass

405   output.

406   A similar conclusion can be drawn for byproduct H_2 from steam cracker plants: The substitution

407   co-product treatment method leads to higher cradle-to-plant-gate GHG emissions than the mass allocation

408   treatment. Despite the co-product treatment methods, the life cycle GHG reduction benefits of all

409   altenative ammonia production pathways using by-product H_2 are robust compared to the conventional

410   SMR pathway.

411   ## Key process parameters

412   In this analysis, the assumptions for key process parameters are shown in Table 2. We assess how

413   varying these parameters within predefined ranges affects the cradle-to-plant-gate GHG emissions of

414   ammonia. Electrolyzer efficiency for H_2-LTE has not been included, since renewable electricity from

415   solar/wind is assumed to power water electrolysis, and thus the efficiency value is inconsequential to

416   GHG emissions.

417   Table 2: Key process parameters and their potential ranges assumed for stochastic analysis

	Assumption	Range	Unit
HB reaction pressure	200	$150 - 250$[5,7]	bar
Pressure drop in the HB loop	6%	$3\% - 10\%$	
Single-pass conversion rate in HB loop	15%	$10\% - 35\%$[7]	
Electricity use for cryogenic ASU	0.2	$0.15 - 0.25$[26]	kWh/m^3
Ammonia condensation temperature	-30	$-25 - -33$[5]	℃

418

419   We randomly sampled each parameter within its corresponding range 2000 times, assuming

420   uniform distribution, and used the sampled values to generate the cradle-to-plant-gate GHG emission

421   results. Figure 6(a) indicates that the assumed ranges of key process parameters lead to a wide range in

422   cradle-to-plant-gate GHG emissions from the N_2-CD and H_2-LTE pathway. The baseline value is 0.221

423   metric ton GHG/metric ton NH_3, as indicated by the dashed line, with a standard deviation of 0.015

424   metric ton GHG/metric ton NH_3. By decreasing the HB reactor pressure, reducing the pressure drop in the

425   HB loop, increasing the single-pass conversion rate, and reducing the electricity consumption per unit of

426   N_2 produced, the cradle-to-plant-gate GHG emission of ammonia can be reduced by 20% to 0.178 metric

427   ton GHG/metric ton NH_3.

428   This is further confirmed by the sensitivity analysis shown in Figure 6(b), which shows the effect

429   of varying each parameter within the specified range, one at a time. In the tornado plot, the x-axis

430   indicates the percentage differences induced by each process parameter as compared to the baseline

431   scenario. For the N_2-CD and H_2-LTE pathway to produce ammonia, the electricity consumed to produce

432   one unit of N_2 is the most influential parameter. This is partly because in this pathway, the life cycle GHG

433   emissions resulting from N_2 production contribute 29% to the life cycle results. Reducing the electricity

434   consumption from 0.2 to 0.15 kWh/m³ N₂ produced can lower the cradle-to-plant-gate GHG emissions by

435   7.3%. Reducing the HB reaction pressure from 200 bar to 150 bar while maintaining the single-pass

436   conversion rate leads to a 6.6% decrease in the cradle-to-plant-gate GHG emissions. Improving the

437   single-pass conversion rate in the HB loop from 15% to 35% would reduce the cradle-to-plant-gate GHG

438   emissions of ammonia production by 4.5%, since a higher single-pass conversion rate would reduce the

439   amount of recycled syngas that needs to be recompressed. A single-pass conversion rate of 35%, instead

440   of 15%, would reduce the size of the recycled syngas stream by two-thirds. Therefore, less energy would

441   be required for recycled syngas recompression, if the single-pass pressure drop in the HB loop remains

442   the same. With a lower single-pass pressure drop, the energy consumption for recycled syngas

443   recompression would be further reduced.
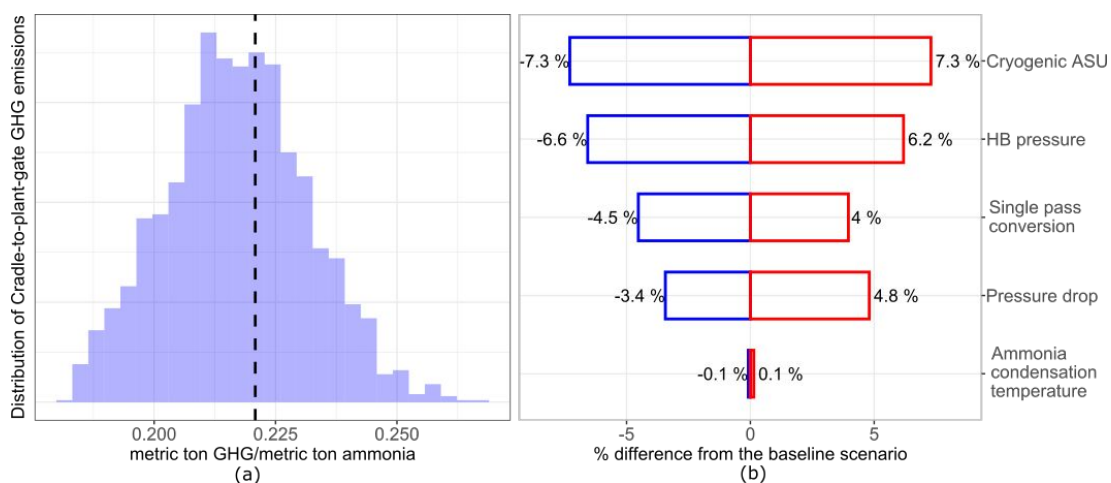
444

445   Figure 6: Impacts of assumptions on key process parameters on the cradle-to-plant-gate GHG emission of ammonia
446   produced via N₂-CD and H₂-LTE.

4. Conclusion

448   In this study, we evaluated various ammonia production pathways in terms of their cradle-to-

449   plant-gate energy use and GHG emissions. Four methods for syngas H₂ production were assessed. LTE

450   using renewable electricity outperforms all other technology pathways for H₂ production with respect to

451   cradle-to-plant-gate GHG emissions of ammonia. However, the successful deployment of this technology

452   may require energy storage to buffer the intermittent renewable electricity, which may negatively impact

453   the economics of low-carbon ammonia production. Sourcing H_2 from HTE with SOEC using nuclear

454   power can produce ammonia with low cradle-to-plant gate GHG emissions similar to sourcing H_2 from

455   LTE using wind/solar electricity, but has the advantage of a steady supply of electricity (i.e., nuclear

456   electricity), which may improve the economics of producing low-carbon ammonia. Utilizing the by-

457   product H_2 from chlorine-alkali and steam cracker plants has the potential to produce ammonia at a large

458   scale. However, the cradle-to-plant gate GHG emission of the ammonia produced depends on the co-

459   product treatment method of by-product H_2. Two methods for syngas N_2 production are assessed: The

460   PSA technology is more energy intensive but has a faster response rate than cryogenic distillation. The

461   life cycle GHG reduction benefits of all altenative ammonia production pathways are robust compared to

462   the conventional SMR pathway.

5. Conflicts of interest

464   There are no conflicts of interest to declare.

6. Acknowledgment

7. References

474   (1)   Giddey, S.; Badwal, S. P. S.; Munnings, C.; Dolan, M. Ammonia as a Renewable Energy

475   Transportation Media. *ACS Sustain. Chem. Eng.* **2017**, *5* (11), 10231–10239.

476   https://doi.org/10.1021/acssuschemeng.7b02219.

477   (2)   Food and Agriculture Organization of the United Nations. *World Fertilizer Trends and Outlook to*

478   *2020 Summary Report*; 2017.

479   (3)   Morgan, E.; Manwell, J.; McGowan, J. Wind-Powered Ammonia Fuel Production for Remote

480   Islands: A Case Study. *Renew. Energy* **2014**, *72*, 51–61.

481   https://doi.org/10.1016/j.renene.2014.06.034.

482   (4)   Liu, X.; Reddi, K.; Elgowainy, A.; Lohse-Busch, H.; Wang, M.; Rustagi, N. Comparison of Well-

483   to-Wheels Energy Use and Emissions of a Hydrogen Fuel Cell Electric Vehicle Relative to a

484   Conventional Gasoline-Powered Internal Combustion Engine Vehicle. *Int. J. Hydrogen Energy*

485   **2020**, *45* (1), 972–983. https://doi.org/10.1016/j.ijhydene.2019.10.192.

486   (5)   Smith, C.; Hill, A. K.; Torrente-Murciano, L. Current and Future Role of Haber–Bosch Ammonia

487   in a Carbon-Free Energy Landscape. *Energy Environ. Sci.* **2020**, 331–344.

488   https://doi.org/10.1039/c9ee02873k.

489   (6)   Bicer, Y.; Dincer, I.; Zamfirescu, C.; Vezina, G.; Raso, F. Comparative Life Cycle Assessment of

490   Various Ammonia Production Methods. *J. Clean. Prod.* **2016**, *135*, 1379–1395.

491   https://doi.org/10.1016/j.jclepro.2016.07.023.

492   (7)   Morgan, E. R.; Manwell, J. F.; McGowan, J. G. Sustainable Ammonia Production from U.S.

493   Offshore Wind Farms: A Techno-Economic Review. *ACS Sustain. Chem. Eng.* **2017**, *5* (11),

494   9554–9567. https://doi.org/10.1021/acssuschemeng.7b02070.

495   (8)   Ammonia—a renewable fuel made from sun, air, and water—could power the globe without

496   carbon | Science | AAAS https://www.sciencemag.org/news/2018/07/ammonia-renewable-fuel-

497   made-sun-air-and-water-could-power-globe-without-carbon (accessed Mar 5, 2020).

498   (9)   Liu, X.; Kwon, H.; Northrup, D.; Wang, M. Shifting Agricultural Practices to Produce

499   Sustainable, Low Carbon Intensity Feedstocks for Biofuel Production. *Environ. Res. Lett.* **2020**, *15*

500   (8), 084014. https://doi.org/10.1088/1748-9326/ab794e.

501   (10)   Johnson, M. C.; Palou-Rivera, I.; Frank, E. D. Energy Consumption during the Manufacture of

502   Nutrients for Algae Cultivation. *Algal Res.* **2013**, *2* (4), 426–436.

503   https://doi.org/10.1016/j.algal.2013.08.003.

504   (11)   Zhang, W. F.; Dou, Z. X.; He, P.; Ju, X. T.; Powlson, D.; Chadwick, D.; Norse, D.; Lu, Y. L.;

505   Zhang, Y.; Wu, L.; Chen, X. P.; Cassman, K. G.; Zhang, F. S. New Technologies Reduce

506   Greenhouse Gas Emissions from Nitrogenous Fertilizer in China. *Proc. Natl. Acad. Sci. U. S. A.*

507   **2013**, *110* (21), 8375–8380. https://doi.org/10.1073/pnas.1210447110.

508   (12)   Bicer, Y.; Dincer, I.; Vezina, G.; Raso, F. Impact Assessment and Environmental Evaluation of

509   Various Ammonia Production Processes. *Environ. Manage.* **2017**, *59* (5), 842–855.

510   https://doi.org/10.1007/s00267-017-0831-6.

511   (13)   Pfromm, P. H. Towards Sustainable Agriculture: Fossil-Free Ammonia. *J. Renew. Sustain. Energy*

512   **2017**, *9* (3), 034702. https://doi.org/10.1063/1.4985090.

513   (14)   Frattini, D.; Cinti, G.; Bidini, G.; Desideri, U.; Cioffi, R.; Jannelli, E. A System Approach in

514   Energy Evaluation of Different Renewable Energies Sources Integration in Ammonia Production

515   Plants. *Renew. Energy* **2016**, *99*, 472–482. https://doi.org/10.1016/j.renene.2016.07.040.

516   (15)   Miura, D.; Tezuka, T. A Comparative Study of Ammonia Energy Systems as a Future Energy

517   Carrier, with Particular Reference to Vehicle Use in Japan. *Energy* **2014**, *68*, 428–436.

518   https://doi.org/10.1016/j.energy.2014.02.108.

519   (16)   Morgan, E. R. Techno-Economic Feasibility Study of Ammonia Plants Powered by Offshore

520   Wind, 2013.

521   (17)   Bicer, Y.; Dincer, I. Life Cycle Assessment of Ammonia Utilization in City Transportation and

522   Power Generation. *J. Clean. Prod.* **2018**, *170*, 1594–1601.

523   https://doi.org/10.1016/j.jclepro.2017.09.243.

524   (18)   Lee, D. Y.; Elgowainy, A. By-Product Hydrogen from Steam Cracking of Natural Gas Liquids

525   (NGLs): Potential for Large-Scale Hydrogen Fuel Production, Life-Cycle Air Emissions

526   Reduction, and Economic Benefit. *Int. J. Hydrogen Energy* **2018**, *43* (43), 20143–20160.

527   https://doi.org/10.1016/j.ijhydene.2018.09.039.

528 (19) Lee, D. Y.; Elgowainy, A.; Dai, Q. Life Cycle Greenhouse Gas Emissions of Hydrogen Fuel

529 Production from Chlor-Alkali Processes in the United States. *Appl. Energy* **2018**, *217* (February),

530 467–479. https://doi.org/10.1016/j.apenergy.2018.02.132.

531 (20) Energy Systems. Argonne National Laboratory. The Greenhouse Gases, Regulated Emissions, and

532 Energy Use in Technologies (GREET) Model https://greet.es.anl.gov/ (accessed Apr 16, 2019).

533 (21) Wang, M.; Elgowainy, A.; Lee, U.; Benavides, Pahola Burnham, A.; Cai, H.; Dai, Q.; Hawkins,

534 T.; Kelly, J.; Kwon, H.; Liu, X.; Lu, Z.; Ou, L.; Sun, P.; Winjobi, O.; Xu, H. Greenhouse Gases,

535 Regulated Emissions, and Energy Use in Transportation Model ® (2019 Excel). USDOE Office of

536 Energy Efficiency and Renewable Energy (EERE) 2019. https://doi.org/10.11578/GREET-Excel-

537 2019/dc.20200706.1.

538 (22) IPCC (Intergovernmental Panel on Climate Change). *Climate Change 2014. Synthesis Report.*;

539 Geneva, Switzerland, 2015.

540 (23) Wang, M.; Elgowainy, A.; Lee, U.; Benavides, P. T.; Burnham, A.; Cai, H.; Dai, Q.; Hawkins, T.

541 R.; Kelly, J.; Kwon, H.; Liu, X.; Lu, Z.; Ou, L.; Sun, P.; Winjobi, O.; Xu, H. *Summary of*

542 *Expansions and Updates in GREET® 2019*; Argonne, IL (United States), 2019.

543 https://doi.org/10.2172/1569562.

544 (24) Araújo, A.; Skogestad, S. Control Structure Design for the Ammonia Synthesis Process. *Comput.*

545 *Chem. Eng.* **2008**, *32* (12), 2920–2932. https://doi.org/10.1016/j.compchemeng.2008.03.001.

546 (25) Aspen Plus. Aspentech.

547 (26) Heinz-Wolfgang, H. *Industrial Gases Processing*; WILEY-VCH Verlag GmbH & Co. KGaA,

548 2008. https://doi.org/10.1002/9783527621248.

549 (27) Lee, D.-Y.; Elgowainy, A. A.; Dai, Q. *Life Cycle Greenhouse Gas Emissions of By-Product*

550 *Hydrogen from Chlor-Alkali Plants*; 2017. https://doi.org/10.2172/1418333.

551 (28) Buttler, A.; Spliethoff, H. Current Status of Water Electrolysis for Energy Storage, Grid Balancing

552 and Sector Coupling via Power-to-Gas and Power-to-Liquids: A Review. *Renew. Sustain. Energy*

553 *Rev.* **2018**, *82* (September 2017), 2440–2454. https://doi.org/10.1016/j.rser.2017.09.003.

554   (29)   Ruth, M. F.; Mayyas, A. T.; Mann, M. K. *Manufacturing Competitiveness Analysis for PEM and*

555   *Alkaline Water Electrolysis Systems*; 2019.

556   (30)   Lampert, D. J.; Cai, H.; Wang, Z.; Keisman, J.; Wu, M.; Han, J.; Dunn, J.; Sullivan, J. L.;

557   Elgowainy, A.; Wang, M.; Keisman, J. *Development of a Life Cycle Inventory of Water*

558   *Consumption Associated with the Production of Transportation Fuels*; Argonne, IL (United

559   States), 2015. https://doi.org/10.2172/1224980.

560   (31)   Dai, Q.; Elgowainy, A.; Kelly, J.; Han, J.; Wang, M. *Life Cycle Analysis of Hydrogen Production*

561   *from Non-Fossil Sources*; 2016.

562